INFLUENŢA TEMPERATURII DE SINTERIZARE ASUPRA PROPRIETĂŢILOR UNOR MATERIALE TITAN-HIDROXIAPATITĂ SINTERIZATE ÎN PLASMĂ CU SCÂNTEIE

INFLUENCE OF SINTERING TEMPERATURE ON THE PROPERTIES OF SOME SPARK PLASMA SINTERED TITANIUM-HYDROXYAPATITE MATERIALS

DORINEL TĂLPEANU[1], MAGDALENA VALENTINA LUNGU[1], DELIA PĂTROI[1*], ANCA COJOCARU[2*]

[1]*National Institute for Research & Development in Electrical Engineering ICPE-CA, 313 Splaiul Unirii, 030138, Bucharest, Romania*

[2] *University POLITEHNICA of Bucharest, Faculty of Applied Chemistry and Materials Science, 1, G. Polizu Str., 011061, Bucharest, Romania*

In this study were achieved advanced materials through the processing of some titanium-hydroxyapatite (Ti-HAp) powders by spark plasma sintering (SPS) technique. The Ti-HAp powders containing 95 wt.% Ti and 5 wt.% HAp were mechanically milled for 40 hours and then sintered at 900°C, 1000°C, and 1075°C for 10 minutes by SPS. The surfaces of the SPSed samples were finished by mirror polishing so that the final sizes were 20±0.05 mm in diameter and 4±0.3 mm in height. The samples were characterized by X-ray diffraction (XRD) and scanning electron microscopy (SEM). The density was determined by Archimedes' method in distilled water, and the mechanical properties were investigated by instrumented indentation testing and Oliver & Pharr method. The surface roughness Ra was determined by contact profilometry. The tribological tests included the measurement of the coefficient of friction (COF) in dry conditions. All sintered samples revealed crystalline phases, homogeneous microstructure, high density (4.45-4.52 g/cm^3), low surface roughness Ra (0.07-0.14 µm), high Vickers hardness (786-879 HV), Young's modulus of 111-137 GPa, elastic contact stiffness between 6.48 N/µm and 6.9 N/µm, and mean COF of up to 0.47. The properties were enhanced with the increase of the sintering temperature due to the advanced features of the SPS technique. Ti-HAp powder sintered at 1075°C revealed the best properties that recommend this material as a promising candidate in the development of medical applications.

În acest studiu s-au obținut materiale avansate prin procesarea unor pulberi de titan-hidroxiapatită (Ti-HAp) folosind tehnica de sinterizare în plasmă cu scânteie (SPS). Pulberile de Ti-HAp, cu un conținut masic de 95 % Ti și 5 % HAp au fost măcinate mecanic timp de 40 ore și apoi sinterizate la 900°C, 1000°C și 1075°C timp de 10 minute prin SPS. Suprafețele probelor obținute prin SPS au fost finisate prin șlefuire, astfel încât dimensiunile finale au avut un diametru de 20±0,05 mm și o înălțime de 4±0,03 mm. Probele au fost caracterizate prin difracție de raze X (XRD) și microscopie electronică de scanare (SEM). Densitatea a fost determinată prin metoda lui Arhimede în apă distilată, iar proprietățile mecanice au fost investigate prin încercări de indentare instrumentată și metoda Oliver & Pharr. Rugozitatea suprafeței Ra a fost determinată prin profilometrie de contact. Testele tribologice au inclus măsurarea coeficientului de frecare (COF) în condiții uscate. Toate probele sinterizate au evidențiat faze cristaline, microstructură omogenă, densitate ridicată (4,45-4,52 g/cm^3, rugozitate redusă a suprafeței Ra (0,07-0,14 µm), duritate Vickers ridicată (786-879 HV), modulul lui Young de 111-137 GPa, rigiditatea de contact elastic între 6,48 N/µm și 6,9 N/µm și COF mediu de până la 0,47. Proprietățile au fost îmbunătățite odată cu creșterea temperaturii de sinterizare, datorită caracteristicilor avansate ale tehnicii SPS. Pulberea de Ti-HAp sinterizată la 1075 °C a prezentat cele mai bune proprietăți, care recomandă acest material a fi un candidat promițător în dezvoltarea aplicațiilor medicale.

Keywords: *titanium, hydroxyapatite, Ti-HAp powders, spark plasma sintering (SPS)*

1. Introduction

Titanium-hydroxyapatite (Ti-HAp) materials are considered to be of great interest for current biomedical applications, especially their use in the field of implantology, due to the superior properties of titanium and the special capacity of hydroxyapatite ($Ca_{10}(PO_4)_6(OH)_2$) to form strong chemical bonds with bone tissues [1]. Also, Ni-free titanium allloys containing ecological and non-allergic alloying elements (i.e. Nb, Zr, Mo, Sn, Si, Ta, Fe) are the most often used materials in medical implants due to their special caracteristics such as Vickers hardness (min. 830 HV), tensile strength (min. 345 MPa), compression strength (min. 250 MPa), modulus of elasticity (min. 60 GPa), high corrosion resistance [2, 3], high biocompatibility, completely inert in the human body and an increased ability to adhere to tissues and bones [4-7].

High corrosion resistance is an essential characteristic in the lifetime of a material used in medical implants. Natural oxides of titanium formed anodically, consisting mainly of titanium dioxide (TiO_2), effectively protect the implant against its rapid dissolution in the rough environments of the human body [8-11]. The surface oxide film allows titanium to show bioactivity in body fluids, providing a storage place for calcium and phosphate compounds, thus inducing ion exchange with apatite in bone tissue [12]. Despite these bioactivities, titanium cannot form strong bonds with mineral bone tissues necessary for a quick fixation in the body (osseointegration) [13-15].

* Autor corespondent/*Corresponding author*,
E-mail: delia.patroi@icpe-ca.ro, anca.cojocaru@chimie.upb.ro

To solve these impediments, hydroxyapatite is often used in dental and orthopedic implants. However, the use of hydroxyapatite in stress-resistant implant applications is limited due to its poor mechanical properties, such as Vickers hardness (min. 5 HV), tensile strength (min. 40 MPa), compression strength (min. 500 MPa), and modulus of elasticity (min. 80 GPa) [4, 16].

Hydroxyapatite has good biocompatibility due to its chemical and crystallographic structure similar to living bone tissue and high bioactivity due to partial resorption and replacement of natural bone shortly after implantation [17, 18]. Composite materials consisting of Ti and HAp will have both the favorable properties of titanium and the bioactivity of hydroxyapatite, but a content of HAp > 30 % in Ti-HAp materials can lead to the brittleness of the materials [7]. Hydroxyapatite-coated titanium is a good alternative to increase bioactivity on the implant surface. However, current production techniques present major problems related to the limitation of the interface between metal and ceramic material [19]. Low adhesion of the ceramic material to the metal often causes the ceramic coating to exfoliate, leading to implant failure. Hydroxyapatite, due to its chemical and crystallographic structure similar to that of mineral bone tissue, seems to be the most suitable for medical implants. However, due to the poor mechanical properties of hydroxyapatite, it is not suitable for medical applications that are subject to mechanical stress [20]. The low modulus of elasticity of titanium and titanium based alloys is widely considered to be a bio-mechanical advantage. The low density of titanium alloys provides a specific strength-to-weight ratio that allows for weaker and stronger structures. Titanium and titanium alloys have relatively low tribological properties due to their poor hardness [21]. However, titanium and titanium alloys are generally considered to have outstanding biocompatibility and high corrosion resistance [22, 23]. The excellent biocompatibility of HAp together with the mechanical properties of Ti make these materials promising candidates in the development of medical applications. There are two main methods to establish a connection between these two materials: the first method is to manufacture sintered materials by powder metallurgy (PM) techniques using Ti and HAp powders [24-26], and the second method is to functionalize the surface of Ti and Ti alloys using HAp as a coating material [27, 28]. Due to the large differences in the physical and thermal properties between Ti and HAp, the first method seems to be more efficient [29,30].

In this study, we present the research results obtained by developing advanced materials through the processing of some Ti-HAp powders by spark plasma sintering (SPS) technique, at different sintering temperatures (900°C, 1000°C, and 1075°C). The SPSed samples were characterized by XRD to identify the phases. The microstructure was analyzed by SEM. Physical, mechanical, and tribological tests were performed to determine the influence of the sintering temperature on the properties of the SPSed samples.

Our study aimed to develop advanced materials with improved properties using Ti-HAp powders that were homogenized by mechanical milling and sintered by an advanced PM technique such as SPS technique.

2. Experimental part

2.1. Preparation of Ti-HAp powder mixture

For the realization of a Ti-HAp powder mixture containing 95 wt.% Ti and 5 wt.% HAp we used a ceramic microcrystalline powder of hydroxyapatite (< 100 μm) synthesized by us by precipitation from aqueous solutions of salts as we described elsewhere [31], and a titanium powder (100-150 μm, purity 99.4%, Merck).

The mechanical milling of the powder mixture was performed in petroleum ether medium using a planetary mill with two workstations (model Retsch PM 400). For an effective milling, stainless steel balls were used, the weight ratio between powders and balls was 1:10, and the rotation speed was 200 rpm for 40 hours.

The Ti-HAp powder obtained from the mechanical milling process was sintered using a spark plasma sintering installation of HP D25 type (FCT Systeme GmbH) equipped with a during current (DC) pulse generator. The milled Ti-HAp powder was introduced into a high-density graphite mold with an inner diameter of 20 mm, 0.4 mm thick graphite foils were placed between the punches and the powder, and to avoid the temperature gradient the mold was coated with graphite felt. The SPS process was performed under vacuum, at a pressing pressure of 50 MPa, DC pulse duration (t_{ON}) of 12 ms, pause duration (t_{OFF}) of 2 ms, additional pause duration (t_P) of 24 ms at 50 Hz, and the number of pulses (n) of 2, the heating/cooling rate was of 50 °C/min, the sintering temperature was 900°C, 1000°C, and 1075°C, and the dwell time was 10 minutes at the maximum temperature. The same amount of Ti-HAp powder was used per each SPSed sample. The surfaces of the SPSed samples were finished by mirror polishing, after the removal of the graphite foils.

The surface condition of the mirror polished samples was determined by measuring the roughness parameter Ra (arithmetic mean deviation of the evaluated profile) with a Surtronic S25 contact profilometer (Taylor & Hobson) for an evaluation length of 4 mm, a cut-off of 0.8 mm, and a digital Gaussian filter.

2.2. Structural analysis by X-ray diffraction

X-ray diffraction investigation was performed by use of a Bruker D8 Discover instrument, in Bragg Brentano geometry, equipped with a 1D LynxEye detector and Cu source radiation, Kα of 1.5406 Å, voltage (U) of 40 kV, intensity (I) of 40 mA, at a scan speed of 1s/step, and an increment of 0.04°. For the crystalline phase analysis was used the ICDD PDF2 Release 2015 database.

2.3. Analysis of microstructure

Scanning electron microscopy (SEM) was used to visualize both the microstructure of the obtained materials and the qualitative distribution of the granular phases and pores in the texture of the materials. The SEM analysis of both powder and sintered materials was performed using a FESEM-FIB Auriga scanning electron microscope and a maximum acceleration voltage of 21 kV.

2.4. Determination of density

The density of the sintered samples was determined according to the standard test methods for density of sintered PM products using Archimedes' principle (ASTM B962) and a Mettler Toledo hydrostatic balance, by successive weighing in air and then in distilled water at a temperature of 23.4°C. For each sample, 3 measurements were made, their mean values being presented.

2.5. Mechanical tests

Mechanical characterization of the sintered samples was performed by instrumented indentation testing (IIT) to determine the Vickers hardness, Young's modulus (E_{IT}), and elastic contact stiffness (S) of the investigated samples, from the indentation curves and Oliver & Pharr calculation method, using a Micro-Combi mechanical tester (CSM Instruments, Switzerland) equipped with a microindentation module (MHT) and a Vickers diamond indenter. The microindentation tests were performed with an indentation load of 20 N, an approach speed of the indenter of 2 μm/min, the duration of keeping the indenter at the maximum load of 15 s, linear loading/unloading speed of 40 N/min, and frequency of data acquisition of 10 Hz. The environmental conditions during the tests were air temperature of 22±3 ºC, and the relative humidity of the air of 32±3 %. On each sample, 5 measurements were performed, their average values being presented, where the load and the indentation depth were measured continuously during the indentation test.

2.6. Tribological tests

The tribological characterization of the sintered samples consisted in the determination of the coefficient of friction in dry conditions. The measurements of the coefficient of friction of the samples were performed with a standard ball-on-disk tribometer equipped with a rotary module (CSM Instruments, Switzerland). The tribological tests were performed in a dry environment at an air temperature of 21±3ºC and a relative air humidity of 43±3 %, using a normal load of 5 N (dead weight) applied on the elastic arm of the tribometer, a linear speed of the sample of 5 cm/s, a sliding distance of 50 m, a sliding radius of 6 mm, and frequency of data acquisition of 0.2 Hz. A 100Cr6 steel ball of 6 mm in diameter mounted on a stiff cantilever was used as a static partner. For each test was used a novel ball to assure a proper solid-solid contact between the sample and the counterpart.

3. Results and discussions

Table 1 presents the values of the sizes and surface roughness Ra of the SPSed samples, after mechanical polishing of the surface of the samples.

Table 1

Sizes and surface roughness Ra of the samples obtained by SPS and mirror surface polished/*Dimensiunile și rugozitatea suprafeței Ra a probelor obținute prin SPS și finisate prin șlefuire*

Sample code	Sintering temperature (ºC)	Diameter (mm)	Height (mm)	Surface roughness Ra (μm)
P1	900	20 ± 0.05	4.1 ± 0.3	0.12 ± 0.02
P2	1000	20 ± 0.05	3.9 ± 0.3	0.10 ± 0.02
P3	1075	20 ± 0.05	3.8 ± 0.3	0.09 ± 0.02

According to the data disclosed in Table 1, it is observed that the samples obtained by SPS technique at various sintering temperatures (900ºC, 1000ºC, and 1075ºC), but at the same pressing pressure (50 MPa) and DC pulse scheme did not yield a shrinkage in diameter. By increasing the sintering temperature, a slight decrease in the height of the samples occurred, even the same amount of Ti-HAp powder was used per each sample.

At visual inspection, all SPSed samples did not show any defects. Moreover, mirror polishing of samples' surfaces led to the achievement of smooth surfaces with low surface roughness Ra values of up to 0.14 μm. Low surface roughness Ra values indicate a good performance of the materials since irregularities and defects on the surfaces can form nucleation sites for corrosion.

3.1. Structural characterization

Figure 1 shows the diffractograms of the samples processed by SPS at temperatures of 900°C, 1000°C, and 1075°C for 10 minutes using Ti-HAp powders that were mechanically milled for 40 hours. The elementary cell parameters, the average crystallite size, and the ratio of crystalline phases were determined by Rietveld analysis and are presented in Table 2.

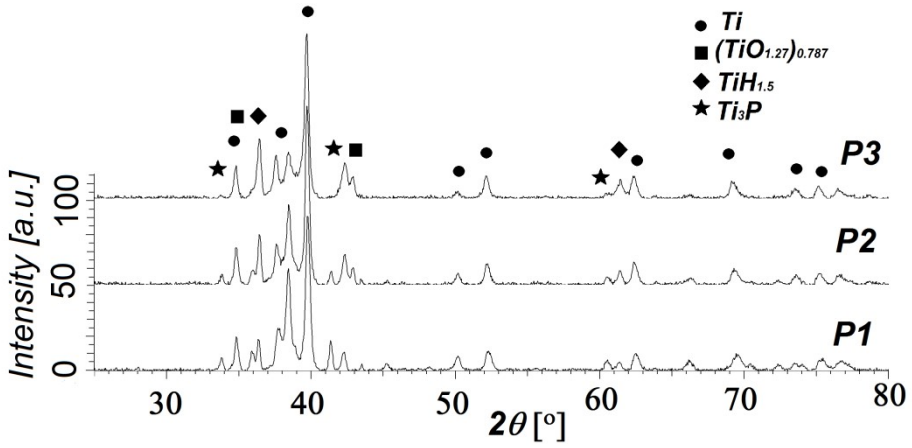

Fig.1 - X-ray diffraction patterns for the samples sintered at 900°C, 1000°C, and 1075°C / *Diagramele de difracție de raze X ale probelor sinterizate la 900°C, 1000°C și 1075°C.*

Table 2

Elemental cell parameters, mean crystallite size and crystal phase content for the samples obtained by SPS and mirror polished/*Parametrii celulei elementare, dimensiunea medie de cristalit și conținutul fazelor cristaline pentru probele obținute prin SPS și finisate prin șlefuire*

Sample code	Sintering temperature (ºC)	Crystalline phase	Crystalline structure	Weight fraction (%)	Lattice parameters (Å)			Mean crystallite size (nm)
					a	*b*	*c*	
P1	900	Ti	hexagonal	50.3	2.97	2.97	4.76	34.0
		$TiH_{1.5}$	triclinic	29.1	4.28	4.21	4.36	42.9
		Ti_3P	tetragonal	5.20	9.77	9.77	5.34	20.0
		$(TiO_{1.27})_{0.787}$	cubic	15.4	4.27	4.27	4.27	15.4
P2	1000	Ti	hexagonal	38.4	2.97	2.97	4.77	41.5
		$TiH_{1.5}$	triclinic	27.5	4.28	4.19	4.36	53.7
		Ti_3P	tetragonal	4.30	9.64	9.64	5.37	12.8
		$(TiO_{1.27})_{0.787}$	cubic	29.8	4.27	4.27	4.27	50.2
P3	1075	Ti	hexagonal	34.9	2.97	2.97	4.78	34.9
		$TiH_{1.5}$	triclinic	35.2	4.27	4.22	4.34	28.4
		Ti_3P	tetragonal	6.10	9.71	9.71	5.33	12.2
		$(TiO_{1.27})_{0.787}$	cubic	23.8	4.27	4.27	4.27	36.8

In the sintered samples were identified crystalline phases resulting from the process of decomposition of hydroxyapatite at high temperatures and its reactivity with Ti [32, 33], respectively Ti oxide having hexagonal and cubic lattice, titanium hydride ($TiH_{1.5}$) with triclinic structure, respectively titanium phosphide (Ti_3P) with tetragonal structure.

From a structural and compositional point of view, the crystallographic phases develop competitively in correspondence with the sintering temperature. At 900ºC the hexagonal Ti phase is predominant, while at 1075ºC the cubic Ti oxide phase is further developing as result of chemical reaction of Ti and decomposed HAp.The elementary cell parameters do not vary significantly with the sintering temperature, their slight variation being due to the residual stress specific to the development of the crystalline phases with the temperature.

Moreover, a high milling time of over 40 h of Ti-HAp powders that were compacted at 600 MPa and sintered at 1150°C for 2 h under an argon atmosphere can lead to the obtaining of a single crystalline phase of α-Ti without the HAp phase or other compounds resulted from HAp decomposition and its reactivity with Ti, being formed a solid solution of Ca in Ti. At 1300°C, Ca is soluble in Ti with at least 0.13% [34]. In the XRD patterns of the samples developed in our study by a fast SPS process, where the sintering temperature of powders consolidated under pressure and DC pulses can be decreased by 200-300°C compared to the sintering temperatures used in conventional PM techniques, was not identified any compound containing Ca. This finding is in agreement with other literature reports [34].

3.2. Morphological characterization

Relatively high porosity and pore size can be an important factor in the capacity of ceramic powders together with titanium powder to obtain a material with improved mechanical properties.

Figure 2 shows the microstructure of the HAp powder sintered at 1100°C composed of sub-micron crystals, well developed and joined together. The granules are rounded and have dimensions of about 44.5 nm in diameter and ~208 nm in length. Between these large granules is a possibly interconnected porosity, formed by large pores of about 200 nm in diameter.

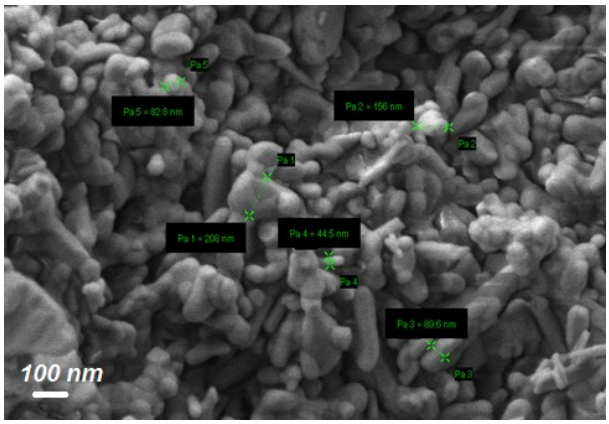

Fig. 2 - SEM image of HAp powder sintered at 1100°C, 100 kX / *Imagine de microscopie electronică (SEM) a pulberii de HAp sinterizată la 1100°C, 100 kX.*

Figure 3 shows the morphology of the titanium powder sintered at 1100°C, which is composed of well-developed sub-micron crystals, but unlike the microcrystalline HAp powder, the microcrystals are no longer fully joined. The granules have irregular shapes, the angles of the edges varying between 45-336 ° and the thickness of the walls is within the range 257-415 nm.

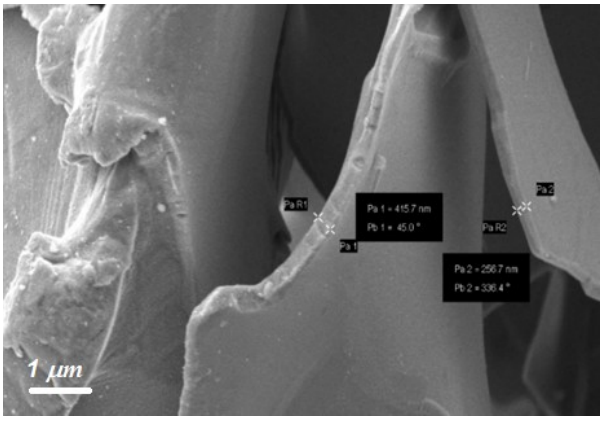

Fig. 3 - SEM images of titanium powder sintered at 1100°C, 20 kX / *Imagine de microscopie electronică (SEM) a pulberii de titan sinterizată la 1100°C, 20 kX.*

Figure 4 and 5 show the morphology of the titanium and hydroxyapatite powder mixture before and after mechanical milling for 40 hours. As can be seen from the SEM images, Ti and HAp particles are clearly differentiated from each other before milling (Fig. 4), but after milling, the Ti-HAp powder has a flake-like morphology (Fig. 5).

Figures 6, 7 and 8 show the micro-structures of the SPSed samples, which highlight the existence of an inherent microporosity of the sintered materials. However, the pores are very small, they have a spherical shape, which indicates that the sintering parameters were selected correctly to achieve dense materials with homogeneous microstructure.

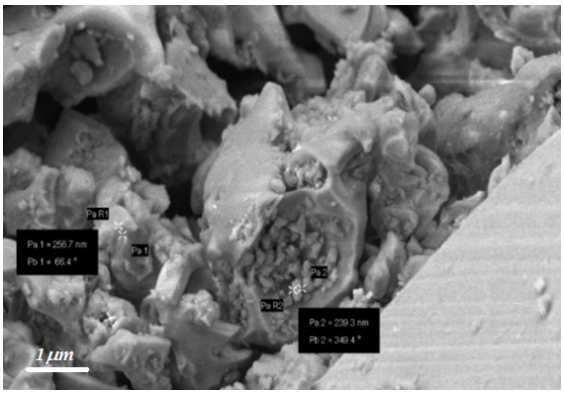

Fig. 4 - SEM image of Ti-HAp powder before milling, 20 kX / *Imagine de microscopie electronică (SEM) a pulberii Ti-HAp înainte de măcinare, 20 kX.*

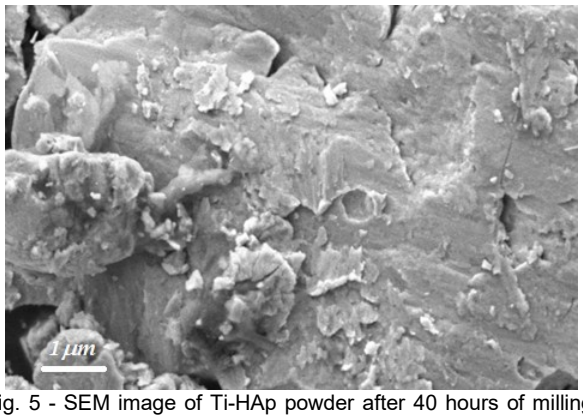

Fig. 5 - SEM image of Ti-HAp powder after 40 hours of milling, 20 kX / *Imagine de microscopie electronică (SEM) a pulberii Ti-HAp după 40 ore de măcinare, 20 kX.*

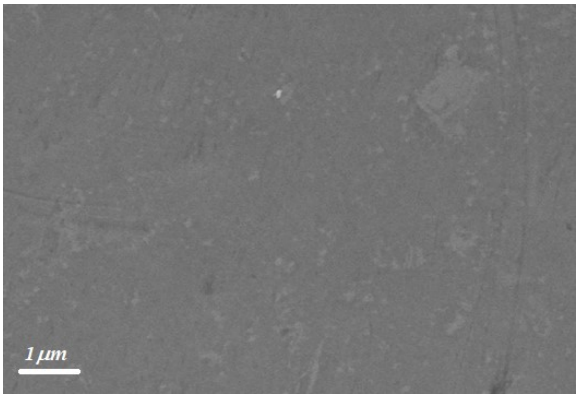

Fig. 6 - Microstructure of Ti-HAp powder sintered at 900ºC, 5 kX / *Imagine de microscopie electronică (SEM) a Ti-HAp sinterizată la 900ºC, 5 kX.*

3.3. Determination of density

The samples obtained by SPS and mirror surface polished exhibited the following mean values of the density: 4.48±0.03 g/cm^3 for the sample P1 sintered at 900°C, 4.49±0.02 g/cm^3 for the sample P2 sintered at 1000°C, and 4.51±0.01 g/cm^3 for the sample P3 sintered at 1075°C. As was expected, the density of the SPSed samples increased with the temperature increase and varied around the theoretical density of Ti (4.5 g/cm^3).

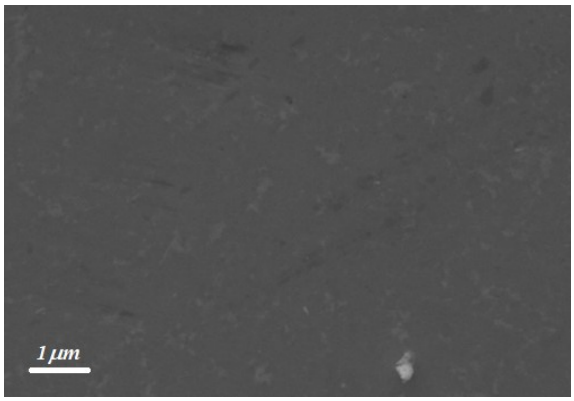

Fig. 7 - Microstructure of Ti-HAp powder sintered at 1000°C, 5 kX / *Imagine de microscopie electronică (SEM) a Ti-HAp sinterizată la 1000ºC, 5 kX.*

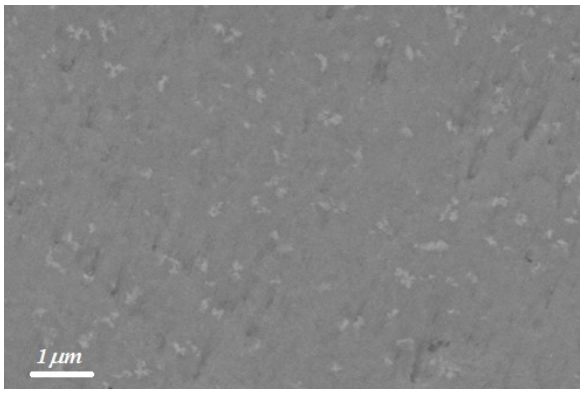

Fig. 8 - Microstructure of Ti-HAp powder sintered at 1075°C, 5 kX / *Imagine de microscopie electronică (SEM) a Ti-HAp sinterizată la 1075ºC, 5 kX.*

Nevertheless, the variation in values is small due to the advanced features of the pressure-assisted and pulsed-current fast sintering process, when an efficient Joule heating occurs throughout the sample material, accompanied by a plastic deformation, as was described elsewhere [35].

3.4. Mechanical testing

Table 3 shows the values of the mechanical properties (Vickers hardness, Young's modulus and elastic contact stiffness) of the samples obtained by SPS and mirror surface polished determined by instrumented indentation testing and Oliver & Pharr calculation method.

All samples yielded good mechanical properties showing hardness of 786-879 HV, Young's modulus of 111-137 GPa, and elastic contact stiffness of 6.48-6.90 N/μm. By increasing the sintering temperature both a densification of the samples and an increase of Vickers hardness are observed, while Young's modulus and elastic contact stiffness decrease. The Ti-HAp powder sintered at 1075°C revealed the best mechanical behavior, showing the highest hardness (864±15 HV) indicating a good resistance to plastic deformation. This material also exhibits the lowest values for Young's modulus (116±5 GPa) and elastic contact stiffness (6.51±0.03 N/μm). These properties are promising to use this material in medical applications (bone or hard tissue implants) since lower values of stiffness or Young's modulus of an implant will not result in bone loss or fracture or in damages of the bone surface [32, 36].

The results obtained in this study are in agreement to the data revealed in other reports [30, 34, 35]. Niespodziana et. al. [34] obtained for Ti-3 vol.% HAp nanocrystalline materials (mechanically alloyed for 44 h, uniaxially pressed at 600 MPa, and sintered at 1150°C for 2 h under an argon atmosphere, having 10 mm in diameter, and 3 mm in height) a Vickers hardness $HV_{0.2}$ of 480 that was greater than the one for Ti (microcrystalline) of 250 $HV_{0.2}$ and HAp (microcrystalline) of 480 $HV_{0.2}$.

Table 3

Vickers hardness, Young's modulus (E_{IT}) and elastic contact stiffness (S) of the samples obtained by SPS and mirror surface polished/*Duritatea Vickers, modulul lui Young și rigiditatea de contact elastic (S) a probelor obținute prin SPS și finisate prin șlefuire*

Sample code	Sintering temperature (ºC)	Vickers hardness HV	Young's modulus (GPa)	Elastic contact stiffness (N/μm)
P1	900	804 ± 18	131 ± 6	6.84 ± 0.06
P2	1000	823 ± 17	128 ± 5	6.63 ± 0.05
P3	1075	864 ± 15	116 ± 5	6.51 ± 0.03

3.5. Tribological tests

Table 4 shows the results of the tribological tests in terms of coefficient of friction (minimum, maximum, mean, and standard deviation) for the samples obtained by SPS and mirror surface polished.

Table 4

Coefficient of friction of the samples obtained by SPS and mirror surface polished/*Coeficientul de frecare al probelor obținute prin SPS și finisate prin șlefuire*

Sample code	Sintering temperature (ºC)	Coefficient of friction (μ)			
		min., μ_{min}	max., μ_{max}	mean, μ_{med}	std. dev.
P1	900	0.066	0.530	0.468	0.042
P2	1000	0.109	0.245	0.180	0.040
P3	1075	0.113	0.174	0.160	0.011

According to the values of the coefficient of friction (COF) obtained for the SPSed samples, it is observed that the sample P1 sintered at 900°C showed the highest mean COF (0.468±0.042), whereas the sample P3 sintered at 1075°C showed the lowest mean COF (0.160±0.011). The sample P2 sintered at 1000°C exhibited also a good tribological behavior, having a low COF (0.180±0.040).

Figures 9, 10 and 11 show the graphs representing the variation of the coefficient of friction with test duration, sliding distance, and number of laps for the tribologically tested samples in dry conditions.

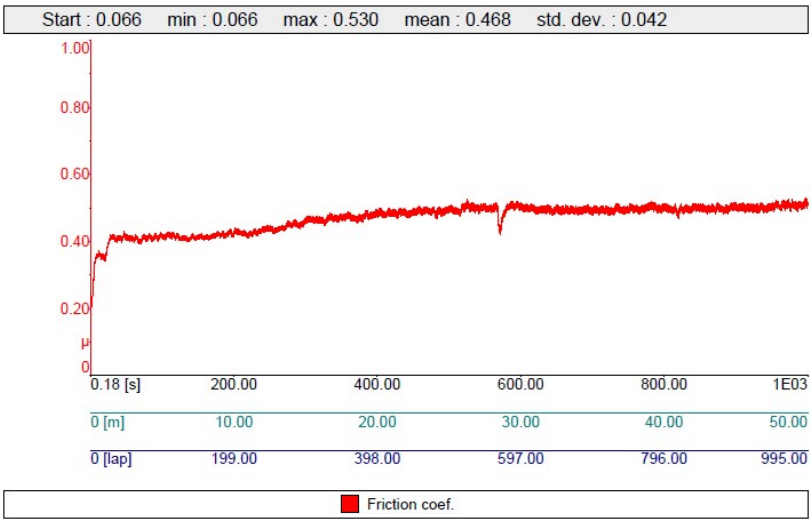

Fig. 9 - Variation of COF with test duration, sliding distance, and number of laps for the sample P1 sintered at 900°C / *Variația COF cu durata testului, distanța de alunecare și numărul de rotații pentru proba P1 sinterizată la 900°C.*

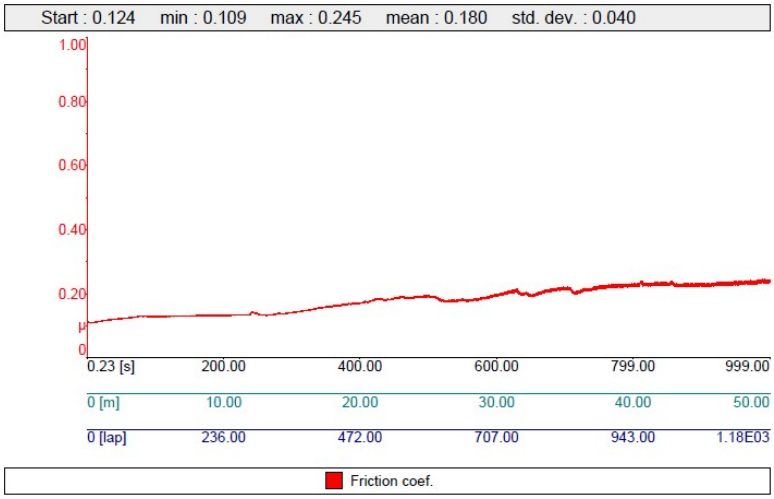

Fig. 10 - Variation of COF with test duration, sliding distance, and number of laps for the sample P2 sintered at 1000°C / *Variația COF cu durata testului, distanța de alunecare și numărul de rotații pentru proba P2 sinterizată la 1000°C.*

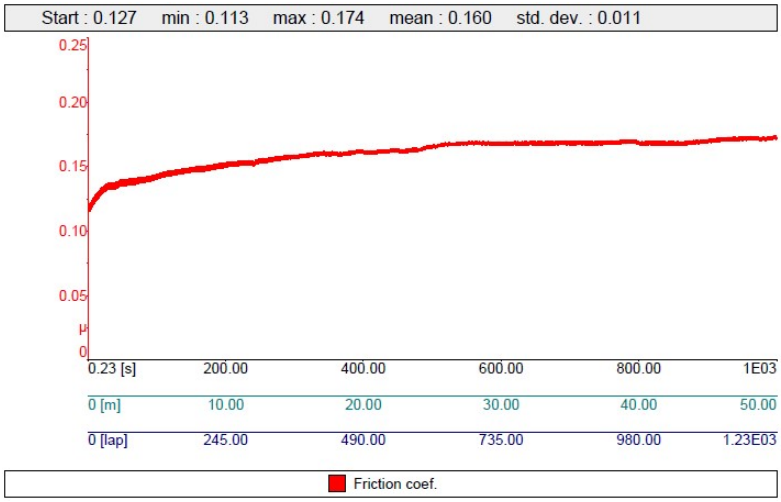

Fig. 11 - Variation of COF with test duration, sliding distance, and number of laps for the sample P3 sintered at 1075°C / *Variația COF cu durata testului, distanța de alunecare și numărul de rotații pentru proba P3 sinterizată la 1075°C.*

As can be noticed in Figure 11, the Ti-HAp powder sintered at 1075°C revealed the best tribological behavior, proved by the variation of COF in a narrow range, where the steady-state was reached after a sliding distance of about 10 m.

The high density of the sintered, homogeneous microstructure and material smooth surfaces (Ra of 0.09±0.02 μm) contributed to the obtaining a low coefficient of friction, along with improved mechanical properties, which in turn will increase the lifetime of the synthesized material.

4. Conclusions

Advanced materials were developed successfully through the SPS processing of Ti-HAp powders containing 95 wt.% Ti and 5 wt.% HAp that were previously mechanically milled for 40 hours. The samples sintered at different temperatures (900°C, 1000°C, and 1075°C) exhibited a crystalline nature, homogeneous microstructure, as well as improved physical, mechanical, and tribological properties due to the advanced features of the SPS technique. The properties were enhanced with the increase of the sintering temperature, the optimum sintering temperature being 1075°C. As a result, the Ti-HAp powder sintered at 1075°C revealed the best properties in terms of density (4.51±0.01 g/cm^3), Vickers hardness (864±15 HV), Young's modulus (116±5 GPa), elastic contact stiffness (6.51±0.03 N/μm), and mean coefficient of friction (0.160±0.011). These properties recommend the developed material as a promising candidate for use in medical applications. However, further studies are necessary to be carried out to prove its biocompatibility.

Acknowledgement

The work has been funded by the bilateral cooperation with JINR DUBNA, theme 04-4-1142-2021/2025, contract 85/2019, pos.35 JINR order 269/2020. The authors acknowledge the technical support of Dr. Eng. Eugen Manta and Drd. Phys. Virgil Marinescu from INCDIE ICPE-CA Bucharest, Romania for performing the density measurements and SEM analysis.

REFERENCES

[1] A. Fahami, R. E.Kahrizsangi, B.N. Tabrizi, Mechanochemical synthesis of hydroxyapatite/titanium nanocomposites, Solid State Sciences, 2011, **13**(1), 135-141.

[2] C.N. Elias, D.J. Fernandes, C.R.S. Resende, J. Roestel, Mechanical properties, surface morphology and stability of a modified commercially pure high strength titanium alloy for dental implants, Dental Materials, 2015, **31**(2), e1-e13.

[3] H.S. Kim, S.J. Yoo, J.W. Ahn, D.H. Kim, W.J. Kim, Ultrafine grained titanium sheets with high strength and high corrosion resistance, Materials Science and Engineering A, 2011, **528**(29-30), 8479-8485.

[4] M. Akao, H. Aoki, K. Kato, Mechanical properties of sintered hydroxyapatite for prosthetic applications, Journal of Materials Science, 1981, **16**, 809-812.

[5] A. Dudek, M. Klimas, The microstructure and selected properties of titanium-hydroxyapatite composites obtained by spark plasma sintering (SPS method), Composites theory and practice, 2013, **13**(3), 208-213.

[6] I-H. Oh, N. Nomura, N. Masahashi, S. Hanada, Mechanical properties of porous titanium compacts prepared by powder sintering, Scripta Mater, 2003, **49**(12), 1197-1202.

[7] C. Popa, V. I. Simon Vida-Simiti, G. Batin, V. Candea, S. Simon, Titanium hydroxyapatite porous structures for endosseous applications, J. Mater. Sci. Mater. Med., 2005,**16**(12),1165-1171.

[8] N. Hayashi, S. Ueno, S.V. Kornarov, E. Kasai, T. Oki, Fabrication of hydroxyapatite coatings by the ball impact process, Surf Coat Technol, 2012, **206**(19-20), 3949-3954.

[9] A.J. Haider, Z.N. Jameel, I.H.M. Al-Hussaini, Review on: titanium dioxide applications, Energy Procedia, Vol. 2019, **157**, 17-29.

[10] A.V. Knyazev, N.G. Chernorukov, E.N. Bulanov, Apatite-structured compounds: Synthesis and high-temperature investigation, Materials Chemistry and Physics, 2012, **132**(2-3), 773-781.

[11] T. Kokubo, Apatite formation on surfaces of ceramics, metals and polymers in body environment, Acta Mater, 1998, **46**(7), 2519-2527.

[12] A.I. Greer, V. Goriainov, J. Kanczler, C.R. Black, L.A. Turner, R.M. Meek, K. Burgess, I. MacLaren, M.J. Dalby, R.O. Oreffo, N. Gadegaard, Nanopatterned titanium implants accelerate bone formation in vivo, ACS applied materials & interfaces, 2020, **12**(30), 33541-33549.

[13] J. Chevalier, L. Gremillard, Ceramics for medical applications: A picture for the next 20 years, Journal of the European Ceramic Society 2009, **29**(7), 1245-1255;

[14] A. Anawati, H. Tanigawa, H. Asoh, T. Ohno, M. Kubota, S. Ono, Electrochemical corrosion and bioactivity of titanium–hydroxyapatite composites prepared by spark plasma sintering, Corrosion Science, 2013, **70**, 212-220;

[15] A. Bigi, N. Nicoli-Aldini, B. Bracci, In vitro culture of mesenchymal cells onto nanocrystalline hydroxyapatite-coated Ti13Nb13Zr alloy, Journal of Biomedical Materials Research A, 2007, **82**(1), 213-221;

[16] Z.X. Li, M. Kawashita, Current progress in inorganic artificial biomaterials, J Artif Organs, 2011, **14**(3), 163-170.

[17] A.Y. Mateus, C.C. Barrias, C. Ribeiro, M.P. Ferraz, F.J. Monteiro, Comparative study of nanohydroxyapatite microspheres for medical applications, Journal of Biomedical Materials Research A, 2008, **86**(2), 483-493.

[18] H. Mehboob, S.-H. Chang, Application of composites to orthopedic prosthesis for effective bone healing: A review, Compos. Struct., 2014, **118**, 328-341.

[19] L.L. Hench, I. Thompson, Twenty-first century challenges for biomaterials, J Roy Soc Interface, 2010, **7**, S379-S391.

[20] K. Bessho, K. Fujimura, T. Iizuka, Experimental long-term study of titanium ions eluted from pure titanium miniplates, Journal of Biomedical Materials Research, 2015, **29**(7), 901-904.

[21] D. He, S. Zheng, J. Pu, G. Zhang, L. Hu, Improving tribological properties of titanium alloys by combining laser surface texturing and diamond – like carbon film, Tribology International, 2015, **82**(A), 20-27.

[22] N. El-Bagoury, S.I. Ahmed, O.A. Abu Ali, S. El-Hadad, A.M. Fallatah, G.A.M. Mersal, M.M. Ibrahim, The influence of microstructure on the passive layer chemistry and corrosion resistance for some titanium-based alloys, Materials, 2019, **12**(8), 1233.

[23] D. Zhao, C. Han, Y. Li, J. Li, K. Zhou, Q. Wei, J. Liu, Y. Shi, Improvement on mechanical properties and corrosion resistance of titanium-tantalum alloys in-situ fabricated via selective laser melting, Journal of Alloys and Compounds, 2019, **804**, 288-298.

[24] A. Arifin, A.B. Sulong, N. Muhamad, J. Syarif, M.I. Ramli, Material processing of hydroxyapatite and titanium alloy (HA/Ti) composite as implant materials using powder metallurgy: A review, Materials & Design, 2014, **55**, 165-175.

[25] N. Omidi, A.H. Jabbari, M. Sedighi, Mechanical and microstructural properties of titanium/hydroxyapatite functionally graded material fabricated by spark plasma sintering, Powder Metallurgy, 2018, **61**(5), 417-427.

[26] M. Jurczyk, K. Niespodziana, K. Jurczyk, Novel Ti-based nanocomposites for medical applications, Obróbka Plastyczna Metali, 2008, **19**(4), 37-45.
[27] S.-J. Ding, Properties and immersion behavior of magnetron-sputtered multi-layered hydroxyapatite/ titanium composite coatings, Biomaterials, 2003, **24**(23), 4233-4238.
[28] M.R. Pantović Pavlović, S.G. Eraković, M.M. Pavlović, J.S. Stevanović, Anaphoretical/oxidative approach to the in-situ synthesis of adherent hydroxyapatite/titanium oxide composite coatings on titanium, Surface and Coatings Technology, 2019, **358**, 688-694.
[29] A. Shahrjerdi, F. Mustapha, M. Bayat, S. M. Saquan, D.L.A. Majid, Fabrication of functionally graded hydroxyapatite-titanium by applying optimal sintering procedure and powder metallurgy, International Journal of Physical Sciences, 2011, **6**(9), 2258-2267.
[30] M. Niinomi, C.J. Boehlert, Titanium alloys for biomedical applications, Advances in metallic biomaterials, 2015, **3**, 179-213.
[31] D. Tălpeanu, A. Cojocaru, R.I. Zamfir (Andronic), M. Bane, S. Ciuca, Comparative tests on resistance to corrosion of some nanocomposites based on titanium hydroxyapatite, U.P.B. Sci. Bull., Series B, 2016, **78**(2), 185-194.
[32] L. Zhang, Z.Y. He, Y.Q. Zhang, Y.H. Jiang, R. Zhou, Rapidly sintering of interconnected porous Ti-HA biocomposite with high strength and enhanced bioactivity, Materials Science and Engineering: C, 2016, **67**, 104-114.
[33] P. Balbinotti, E. Gemelli, G. Buerger, S.A. de Lima, J. de Jesus, N.H. Almeida Camargo, V.A. Rodrigues Henriques, G.D. de Almeida Soares, Microstructure development on sintered Ti/HA biocomposites produced by powder metallurgy, Materials Research, 2011, **14**(3), 384-393.
[34] K. Niespodziana, K. Jurczyk, J. Jakubowicz, M. Jurczyk, Fabrication and properties of titanium–hydroxyapatite nanocomposites, Materials Chemistry and Physics, 2010, **123**(1), 160-165.
[35] M.V. Lungu, E. Enescu, D. Tălpeanu, D. Pătroi, V. Marinescu, A. Sobetkii, N. Stancu, M. Lucaci, M, Marin, E. Manta, Enhanced metallic targets prepared by spark plasma sintering for sputtering deposition of protective coatings, Materials Research Express, 2019, **6**(7), 076565.
[36] Z.Q. Yao, Y. Ivanisenko, T. Diemant, A. Caron, A. Chuvilin, J.Z. Jiang, R.Z. Valiev, M. Qi, H.-J. Fecht, Synthesis and properties of hydroxyapatite-containing porous titania coating on ultrafine-grained titanium by micro-arc oxidation, Acta Biomaterialia, 2010, **6**(7), 2816-2825.

****